CASE REPORT

OPEN

Intraparenchymal Neuromonitoring of Cerebral Fat Embolism Syndrome

Ryan Leo Hoiland, PhD[1,2]

Donald E. Griesdale, MD, MPH[1,3,4]

Peter Gooderham, MD[5]

Mypinder S. Sekhon, MD, PhD[3]

OBJECTIVES: We aimed to characterize the cerebrovascular physiology of cerebral fat embolism using invasive multimodal neuromonitoring.

DATA SOURCES: ICU, Vancouver General Hospital, Vancouver, BC, Canada.

STUDY SELECTION: Case report.

DATA EXTRACTION: Patient monitoring software (ICM+, Cambridge, United Kingdom), clinical records, and surgical records.

DATA SYNTHESIS: None.

CONCLUSIONS: Our integrated assessment of the cerebrovascular physiology of fat embolism syndrome provides a physiologic basis to investigate the importance of augmenting mean arterial pressure to optimize cerebral oxygen delivery for the mitigation of long-term neurologic ischemic sequelae of cerebral fat embolism.

KEY WORDS: brain hypoxia; brain tissue oxygenation; cerebral fat embolism; fat embolism syndrome; mean arterial pressure; neuromonitoring

Fat embolism syndrome (FES) is characterized by neurologic, pulmonary, and cutaneous manifestations (1). CNS manifestations include coma stemming from encephalopathy in the setting of diffuse cerebral microhemorrhages, ischemia, edema, and infarct (1). The cerebrovascular pathophysiology of FES is poorly understood and effective critical care management interventions have remained elusive. Herein, we report the temporal and longitudinal relationships between mean arterial pressure (MAP) and brain tissue oxygenation ($Pbto_2$) in two critically ill cerebral FES patients. Both patients provided written informed consent for inclusion in this case study.

Patient 1 was a 27-year-old female with bilateral femur fractures following a motor vehicle accident. Initial Glasgow Coma Score (GCS) was 15 with no other injuries. Operative fixation was undertaken 30 hours later, and she was extubated with normal consciousness. Her GCS deteriorated to 6T (E1, VT, M4) 24 hours later, and she developed a petechial rash on her torso. Patient 2 was a 22-year-old male with a right femur fracture following a motorcycle accident. His initial GCS was 15. He was intubated for hypoxemic respiratory failure stemming from associated pulmonary contusions. He underwent operative femur fixation 26 hours following injury. Postoperatively, he had normal consciousness but deteriorated to GCS 3T (E1, VT, M1) 30 hours later. For both patients, head MRI (1.5T Siemens, Munich, Germany) confirmed cerebral FES (2) with bilateral extensive restricted diffusion and diffuse punctate hemorrhages (**Fig. 1*A–C***). Thereafter, intracranial pressure (ICP) (Camino; Integra Lifesciences, Princeton, NJ) and $Pbto_2$ (Licox; Integra Lifesciences) microcatheters were inserted into the right frontal lobe via a dual lumen cranial access bolt. Post-neuromonitoring head CT confirmed $Pbto_2$

DOI: 10.1097/CCE.0000000000000396

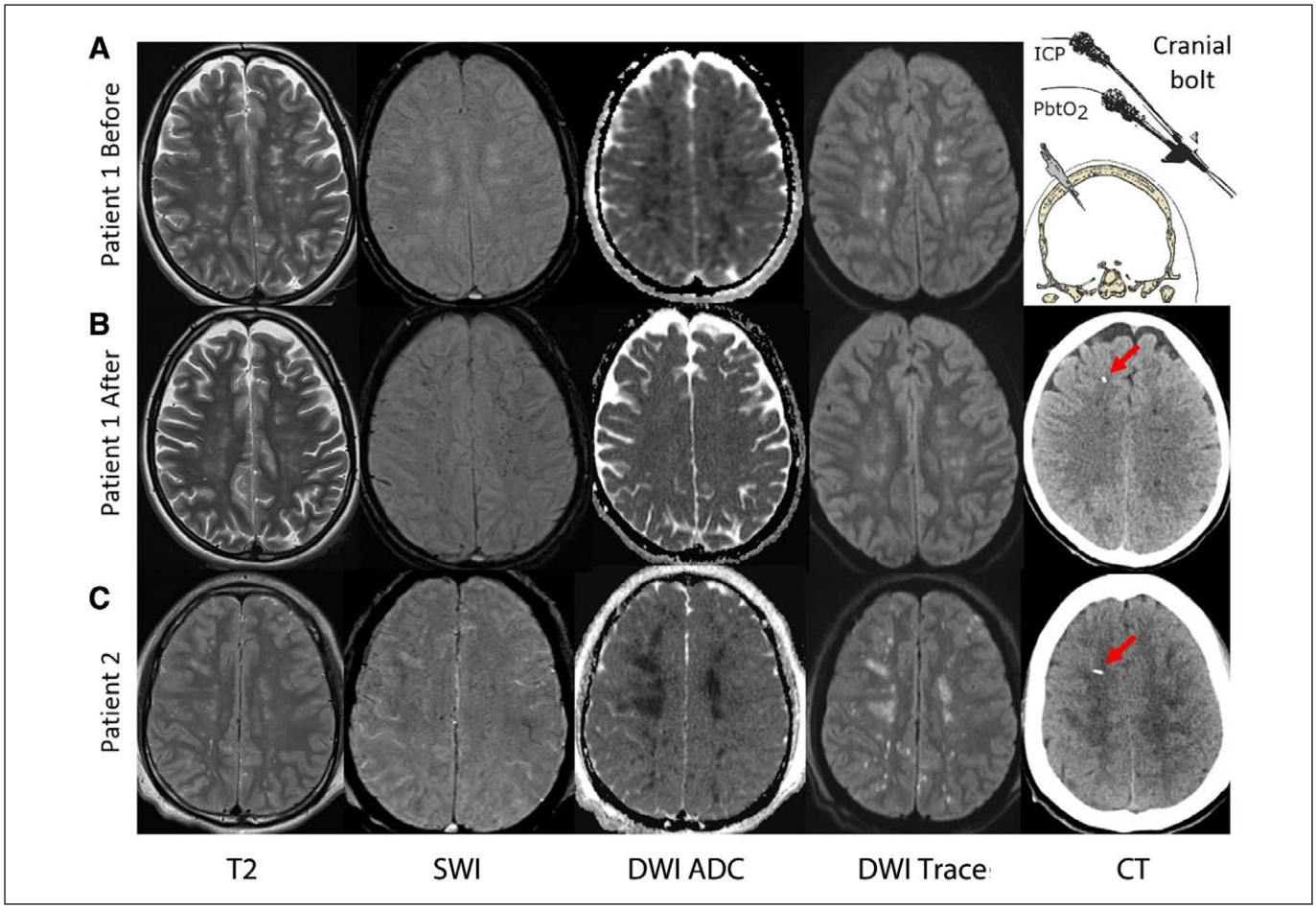

Figure 1. Neuroimaging from both patients including (from *left* to *right*), the axial images for MRI sequences pertaining to T2, SWI, apparent diffusion coefficient (ADC), and diffusion-weighted imaging (DWI) are shown. Collectively, the images in (**A**) reflect bilateral subcortical restricted diffusion (ADC and DWI), reflecting possible tissue ischemia in the setting of fat embolism syndrome. Bilateral diffuse punctate hemorrhages are shown on SWI imaging. In patient 1 and 2, the tip of the brain tissue oxygenation ($Pbto_2$) catheter was confirmed within the tissue region of the MRI confirmed restricted diffusion (denoted by the *red arrow* on noncontrast CT, *rightmost* image in [**B**]). **B**, MRI sequences following goal-oriented management guided by invasive neuromonitoring and after removal of the invasive neuromonitoring days after initiation. The follow-up ADC and DWI sequences reveal partial resolution of the restricted diffusion after neuromonitoring guided care. The SWI sequence does not demonstrate new or increased punctate hemorrhages. **C**, MRI sequences pertaining to T2, SWI, ADC, and DWI images revealing bilateral subcortical white matter restricted diffusion (ADC and DWI) and punctate hemorrhages (SWI) in patient 2. ICP = intracranial pressure, SWI = susceptibility weighted imaging.

catheter positioning within the corresponding region of white matter restricted diffusion (Fig. 1 *A*–*C*). MAP and $Pbto_2$ were continuously recorded at 300 Hz (ICM+, Cambridge, United Kingdom).

In patient 1, neuromonitoring commenced 84 hours following injury, 30 hours after neurologic symptoms and 12 hours after MRI. A post-neuromonitoring head MRI in patient 1 revealed resolution of restricted diffusion in subcortical white matter (**Fig. 1*B***). There were no differences in the degree of punctate hemorrhages following neuromonitoring (Fig. 1*B*). In patient 2, neuromonitoring commenced 72 hours following injury, 16 hours after neurologic symptoms and 6 hours after MRI. There was no follow-up MRI in patient 2.

In both cases, concordant increases in $Pbto_2$ and MAP were apparent with elevated norepinephrine doses longitudinally (**Fig. 2*A*–*D***). In patient 1 ($r = 0.46$; $p < 0.001$) and patient 2 ($r = 0.25$; $p < 0.001$), MAP and $Pbto_2$ were significantly correlated during the monitoring periods. These relationships were supported by near-instantaneous temporal fluctuations in MAP mirrored by concordant changes in $Pbto_2$ (**Fig. 2*C*–*F***). The ICP was consistently less than 20 mm Hg in both cases. We did not observe temporal correlations between improvements in consciousness and resolution of brain hypoxia;

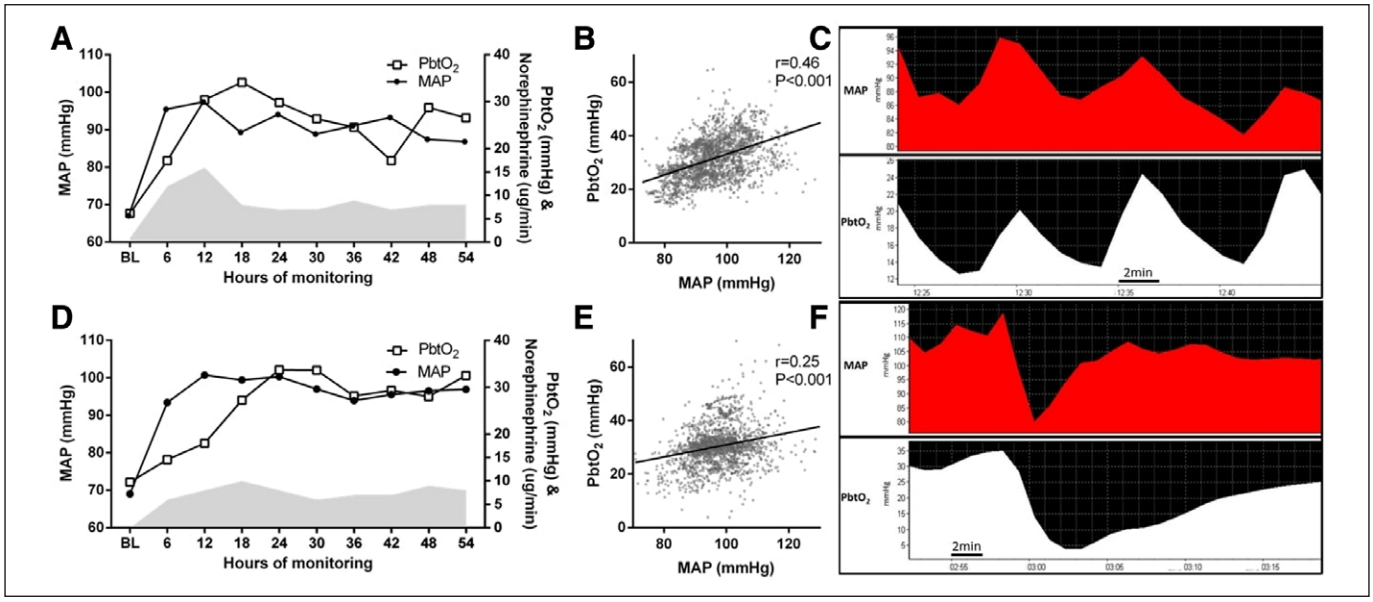

Figure 2. Physiologic neuromonitoring data in both patients demonstrates a link between mean arterial pressure (MAP) and brain tissue oxygenation ($Pbto_2$). **A**–**C**, Neuromonitoring data from patient 1. **A**, Longitudinal data pertaining to MAP and $Pbto_2$ over the first 48 hr of neuromonitoring. The *shaded area* represents the norepinephrine dose longitudinally. **B**, A scatterplot for individual 1-min data points for MAP and $Pbto_2$ in patient 1 with the *dark line* representing the linear regression. **C**, The relationship between MAP fluctuations and changes in $Pbto_2$ in real time during neuromonitoring. As patient 1's MAP decreases less than 90 mm Hg, the patient exhibits episodes of brain hypoxia ($Pbto_2 < 20$ mm Hg). **D**–**F**, Neuromonitoring data from patient 2. **D**, Longitudinal data pertaining to MAP and $Pbto_2$ over the first 48 hr of neuromonitoring. The *shaded area* represents the norepinephrine dose longitudinally. **E**, A scatterplot for individual 1-min data points for MAP and $Pbto_2$ in patient 2 with the *dark line* representing the linear regression. **F**, The relationship between MAP fluctuations and changes in $Pbto_2$ in real time during neuromonitoring. As patient 2's MAP decreases less than 90 mm Hg, the patient exhibits a severe episode of brain hypoxia ($Pbto_2$ ~ 5 mm Hg) with subsequent resolution once MAP is augmented again. In patient 1, the initial neurophysiologic values were intracranial pressure (ICP): 6 mm Hg, MAP 67 mm Hg, cerebral perfusion pressure 61 mm Hg, and $Pbto_2$ 6 mm Hg, while the initial arterial blood gas was pH 7.44, $Paco_2$ 41 mm Hg, and Pao_2 168 mm Hg with a Fio_2 30%. The hemoglobin and sodium concentrations were 105 g/L and 142 mEq/L, respectively. In patient 2, the initial neurophysiologic values were ICP 19 mm Hg, MAP 69 mm Hg, cerebral perfusion pressure 50 mm Hg, and $Pbto_2$ 10 mm Hg, while the initial arterial blood gas was pH 7.48, $Paco_2$ 36 mm Hg, and Pao_2 161 mm Hg with Fio_2 40%. The hemoglobin and sodium concentrations were 79 g/L and 136 mEq/L, respectively. BL = baseline.

however, there were likely significant residual effects of IV sedatives confounding the neurologic examination. Both patients experienced full neurologic recovery at 6 months.

We demonstrate significant relationships between MAP and $Pbto_2$ in two cases of cerebral FES, thereby linking augmented cerebral oxygen delivery to improved brain oxygenation. Analogous to other brain injuries (e.g., traumatic brain injury [3] and cardiac arrest [4]), neuromonitoring guided MAP augmentation was associated with the restoration of brain normoxia ($Pbto_2 > 20$ mm Hg) at targets higher than routinely prescribed in critical care (65 mm Hg).

The pathogenesis of cerebral FES is theorized to result from physical occlusion or diffuse cerebrovascular inflammation (1), culminating in ischemia and cytotoxic edema represented on MRI by restricted diffusion, with progression to infarct without supportive care and/or intervention (1). A systematic review by Kuo et al (5) demonstrated that restricted diffusion is less prevalent in the subacute and late stages of FES. However, an important consideration is that these data are derived from distinct patients at distinct time points (inter-patient comparisons) and therefore cannot be taken to represent an intra-patient time course of FES. Further, at time points ranging from 10 to 15 days postischemic injury, pseudonormalization of the diffusion-weighted imaging signal must be considered when interpreting these neuroimaging results. Other investigations have observed incomplete resolution of cerebral lesions (e.g., Fluid Attenuation Inverted Recovery hyperintensities) as well as long-term neurologic deficits (6).

Our cases suggest cerebral FES-associated restricted diffusion is not indicative of irreversible damage, but rather the tissue may recover with optimization of

cerebral oxygen delivery. In both cases, initial $Pbto_2$ reflected brain hypoxia at conventional MAP targets (65 mm Hg). However, in both patients, we demonstrate an association between increased MAP and resolution of brain hypoxia. In patient 1, we demonstrate significant resolution of white matter restricted diffusion within 5 days post FES diagnosis, which is early enough in the clinical course that pseudonormalization likely does not explain these changes. Importantly, FES patients with restricted diffusion on MRI are known to recover neurologically, and as such, our cases should not be interpreted to imply causation between improved neurologic outcome solely based upon MAP augmentation. Our temporal data highlights instantaneous changes between MAP and $Pbto_2$, emphasizing the dynamic nature of FES cerebrovascular physiology. Finally, our data suggest resolution of brain hypoxia at MAP targets (90 mm Hg) significantly higher than current standards of critical care, thereby suggesting future studies should focus on evaluating the roles of increased MAP targets and goal-oriented therapy in cerebral FES.

Collectively, this integrated assessment of the cerebrovascular physiology of FES provides a physiologic basis to investigate the importance of optimizing cerebral oxygen delivery in prospective studies and trials for the mitigation of long-term neurologic ischemic sequelae of cerebral FES.

1 *Department of Anaesthesiology, Pharmacology and Therapeutics, Vancouver General Hospital, University of British Columbia, Vancouver, BC, Canada.*

2 *Department of Cellular and Physiological Sciences, Faculty of Medicine, University of British Columbia, Vancouver, BC, Canada.*

3 *Division of Critical Care Medicine, Department of Medicine, Vancouver General Hospital, University of British Columbia, Vancouver, BC, Canada.*

4 *Centre for Clinical Epidemiology and Evaluation, Vancouver Coastal Health Research Institute, University of British Columbia, Vancouver, BC, Canada.*

5 *Division of Neurosurgery, Department of Surgery, Vancouver General Hospital, University of British Columbia, University of British Columbia, Vancouver, BC, Canada.*

Dr. Hoiland is funded by a Michael Smith Foundation for Health Research Trainee Fellowship, University of British Columbia Bluma Tischler Post-Doctoral Fellowship, and the Darin Daniel Green Memorial Scholarship. Dr. Griesdale is funded through a Health Professional-Investigator Award from the Michael Smith Foundation for Health Research. Dr. Sekhon is funded through the Vancouver Coastal Health Research Institute Clinician Scientist Award and holds a project grant from the Canadian Institutes of Health Research. Dr. Gooderham has disclosed that he does not have any potential conflicts of interest.

For information regarding this article, E-mail: mypindersekhon@gmail.com

REFERENCES

1. Godoy DA, Di Napoli M, Rabinstein AA: Cerebral fat embolism: Recognition, complications, and prognosis. *Neurocrit Care* 2018; 29:358–365
2. Eguia P, Medina A, Garcia-Monco JC, et al: The value of diffusion-weighted MRI in the diagnosis of cerebral fat embolism. *J Neuroimaging* 2007; 17:78–80
3. Jaeger M, Dengl M, Meixensberger J, et al: Effects of cerebrovascular pressure reactivity-guided optimization of cerebral perfusion pressure on brain tissue oxygenation after traumatic brain injury. *Crit Care Med* 2010; 38:1343–1347
4. Sekhon MS, Gooderham P, Menon DK, et al: The burden of brain hypoxia and optimal mean arterial pressure in patients with hypoxic ischemic brain injury after cardiac arrest. *Crit Care Med* 2019; 47:960–969
5. Kuo KH, Pan YJ, Lai YJ, et al: Dynamic MR imaging patterns of cerebral fat embolism: A systematic review with illustrative cases. *AJNR Am J Neuroradiol* 2014; 35:1052–1057
6. Dunkel J, Roth C, Erbguth F, et al: Cerebral fat embolism: Clinical presentation, diagnostic steps and long-term follow-up. *Eur Neurol* 2017; 78:181–187